Effects of Annealing on the Surface Composition and Morphology of PS/PMMA Blend

C. Ton-That, A. G. Shard, R. Daley, and R. H. Bradley*

Materials Surfaces and Interfaces Group, School of Applied Sciences, The Robert Gordon University, St Andrew Street, Aberdeen AB25 1HG, United Kingdom

Received May 8, 2000; Revised Manuscript Received July 31, 2000

ABSTRACT: Films of polystyrene (PS) and poly(methyl methacrylate) (PMMA) blend have been annealed at a temperature above their glass transition temperatures for up to 48 h. Surface chemical compositions of the cast and annealed films were measured by X-ray photoelectron spectroscopy (XPS) while surface topographical changes were followed by atomic force microscopy (AFM). The blend films spin-cast from chloroform produce nonequilibrium surfaces with a significant excess of PMMA. The polymer component with a lower surface free energy, PS, is shown to segregate to the surface upon annealing. The PS surface concentration of the films, containing 50% PS:50% PMMA in the bulk, was evaluated using the ester peak in XPS C 1s spectra (sampling depth ~ 9 nm) and found to increase from ~5% (freshly spin-cast film) to a saturated level of ~47% after 17 h of annealing. AFM imaging reveals evolution of blend morphology with annealing time. The spin-cast films prior to annealing exhibit pitted topography with typical pit size of ~1.2 μm and depth of 30−40 nm. As the annealing process proceeds, these pits get continually shallower. Frictional force microscopy with hydroxylated tips recorded surface phase separations for the films of 2−4 h annealing. As the annealing continues to above 14 h, the pitted structure becomes distorted. The surface enrichment and morphology changes upon annealing are explained by dewetting of PMMA relative to PS.

Introduction

A number of technologically important properties of polymeric materials are controlled by their surface chemistry and morphology. Examples are the contact angle with liquids, corrosion resistance, and frictional properties of the materials. For polymer blends or block copolymers, the composition at the surface is often different from the bulk composition due to larger thermal molecular motions of polymer chains in the surface region.[1] In an equilibrium binary blend system with similar molecular weights for each component, one would expect the lower free energy component to be enriched at the surface to reduce the total surface energy. This phenomenon of surface enrichment has been reported for the blend systems of polycarbonate (PC)/poly(methyl methacrylate) (PMMA),[2,3] poly(ethylene-*co*-propylene) (PEP)/polystyrene (PS),[4] and poly(ethyl acrylate) (PEA)/poly(vinylidene fluoride-*co*-hexafluoroacetone) (PVDF−HFA).[5] Surface morphology is another important aspect of polymer blends. Both grains/matrix and holes/matrix morphologies have been observed, depending on the blend compositions[6−8] and film thickness.[9,10]

For incompatible polymers, the surface morphology and composition of their solvent-cast blends can be modified by different factors such as casting solvent,[2,11] temperature,[12] and chain end groups.[13] Solvent-cast blends from volatile solutions such as chloroform or toluene may not be thermodynamically equilibrated due to rapid solvent evaporation during the spin-casting process, and the resulting surface could primarily be the result of solvent effects.[14,15] These solvent effects may be removed or at least reduced by annealing the cast films under appropriate conditions. It has been found that solvent-cast films of PS/deuterated PS (dPS) blend, the latter of which has a slightly lower surface tension, tended to produce nonequilibrium surfaces with a high concentration of PS, whereas annealing resulted in a surface excess of dPS.[16−18] These and similar[13,19,20] studies have demonstrated the effects of annealing on the surface composition of blends and block copolymers, the component with lower surface free energy preferentially segregating to the surface. Previously, we have described the surface analysis of PS/PMMA blends spin-cast from chloroform solution.[7] X-ray photoelectron spectroscopy (XPS) measurements revealed that the PMMA component was enriched at the surface although it has a slightly higher surface free energy. In this study, the blend films have been annealed at a temperature above their glass transition temperatures, and measured changes in surface composition and topography upon annealing are presented. In addition, we have employed chemically modified AFM probe tips to probe the phase structure of the film surfaces via the polar and nonpolar natures of PMMA and PS, respectively.

Experimental Section

Polystyrene (PS) (M_w = 100 000) and poly(methyl methacrylate) (PMMA) (M_w = 120 000) were used as obtained (Sigma Aldrich, UK). Glass transition temperatures of the PS and PMMA, measured by differential scanning calorimetry, were 106 and 111 °C (±2 °C), respectively. Polymer solutions were prepared by dissolving a composition of 50% PS and 50% PMMA (weight percent) in chloroform to obtain 1% weight/volume solution. Polymer films were prepared by spin-casting 60 μL aliquots of the polymer solutions under ambient conditions onto a freshly cleaved mica substrate, which was rotated at ~3000 rpm for 2 min. Film thickness was evaluated by scratching through the polymer film down to the substrate using stiff AFM cantilevers and high loading force, as described previously.[21] The average thicknesses of the cast film were measured at ca. 65 ± 11 nm. The films were subsequently annealed at 142 ± 6 °C in a vacuum oven (pressure < 10 Torr)

* Corresponding author. Phone (44.1224) 262822; Fax (44.1224) 262828; E-mail r.bradley@rgu.ac.uk.

10.1021/ma000792h CCC: $19.00
Published on Web 10/12/2000

for various durations. The samples were removed periodically and quenched to room temperature for analysis.

Surface chemical compositions of the films were measured by XPS using a Kratos Axis 5-channel HSi spectrometer with monochromated Al Kα (1486.6 eV) X-rays operated at 150 W. The sample analysis chamber of the XPS instrument was maintained at a pressure of $\sim 4 \times 10^{-9}$ Torr. Charge neutralization was used for all the samples to offset charge accumulation with standard operating conditions for insulator surfaces, −2.8 V bias voltage, −1.0 V filament voltage, and +1.9 A filament current. Elemental compositions were calculated from the areas of carbon 1s (C 1s) and oxygen 1s (O 1s) peaks in the survey spectra, which were collected at a pass energy of 80 eV, using appropriate relative sensitivity factors. Error for peak area analysis was estimated at ±5 at. %, deduced from elemental analysis of PTFE. Detailed surface chemical composition was obtained by analysis of C 1s envelopes collected at a pass energy of 20 eV. Chemical shift peaks are charge referenced to the C−C/C−H peak at 285 eV. Peak analysis was carried out using Kratos software and also version 1.5 of the Spectral Data processor (XPS International). Surface topography of the films was characterized by AFM under ambient conditions, using a Digital Instruments (DI) Multimode SPM IIIa system. All imaging was performed in tapping mode using silicon tips with cantilever driving amplitudes of 45−80 nm and feedback achieved at ∼60% of the driving amplitude. Image analysis was performed using commercial DI software (version 4.23r3).

To probe phase structure on the polymer blend surfaces, AFM tips bearing hydrophilic hydroxyl groups were employed. Procedures for cleaning and hydrophilization of the AFM tips were carried out in accordance with the prescription of Ito et al.[22] The Si_3N_4 cantilevers with integrated tip were exposed to an ultraviolet ozone (UVO) for 15 min in a Jelight 42-220 UVO cleaner. UVO treatment has been shown to effectively remove contaminants such as hydrocarbons[23] and will further oxidize the native oxide layer on the Si_3N_4 tip surface. After UVO treatment, the tips were first immersed in 0.5 M NaOH for 20 min, then in 0.1 M HCl for 10 min, and finally in 0.5 M NaOH for 10 min. Subsequently, the tips were rinsed in Milli-Q deionized water (resistivity = 18.3 MΩ cm) and dried in a vacuum for 10 min at 100 °C. This procedure has been reported to make the tip surface become more hydrophilic by increasing the surface concentration of silanol groups.[22,24] The water contact angles have also been measured on model Si_3N_4 wafers to drop from 60° to 18° (±3°) after such treatment. The hydroxylated tips and wafers have a high surface energy and are thus easily contaminated. However, the hydroxylated wafers that had been stored for 2 weeks in closed containers under air had the contact angles indistinguishable from those determined immediately after treatment. In the present experiments, the tips were used immediately after treatment to minimize surface contamination.

Frictional force microscopy (FFM) imaging was performed simultaneously with topographical imaging in contact mode by scanning the tip in the direction orthogonal to the long cantilever axis. The probes used were standard 200 μm long V-shaped Si_3N_4 cantilevers with narrow legs (nominal spring constant 0.06 N m^{-1}, nominal tip radius 20−60 nm[25]). A constant scan rate of 6 μm s^{-1} was used in all the FFM experiments. The possible influence of capillarity was removed by undertaking all lateral force imaging under fluid.[26] Decane ($C_{10}H_{22}$) was chosen as the medium for all FFM experiments due to its nonpolarity, which also eliminates any electrostatic double-layer interaction forces between the polymer surface and probe tip.[27] In addition, it is a nonsolvent for both of the polymers and convenient to use in AFM experiments because of its high boiling point (174 °C) and low toxicity.

Results

X-ray Photoelectron Spectroscopy (XPS). XPS survey spectra of the spin-cast films demonstrate the presence of only two elements, carbon and oxygen, with no signals indicative of the mica substrate being present.

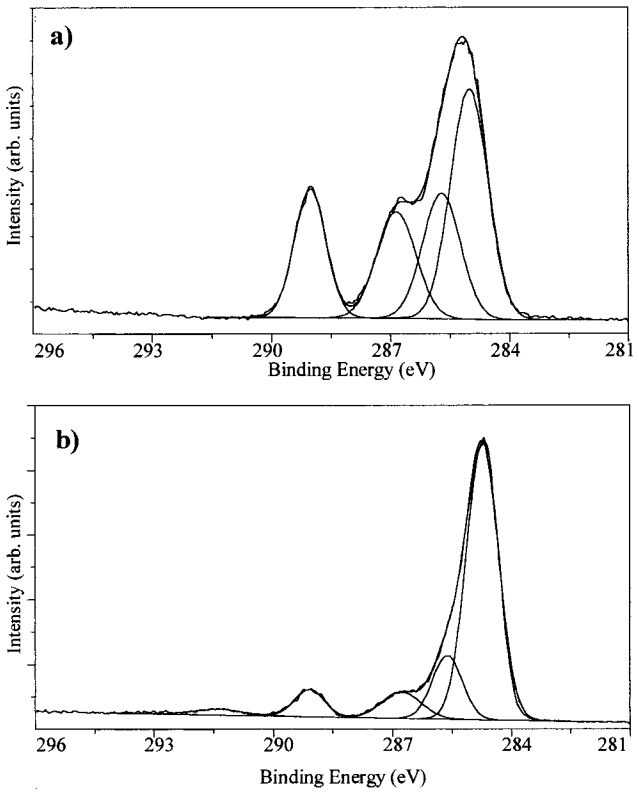

Figure 1. High-resolution C 1s spectra with fitted curves for spin-cast 50% PS:50% PMMA film (a) and after 42 h annealing (b).

In some of the annealed samples, silicon signals were detectable though not significant. The absence of aluminum signal (Al 2p ∼ 74 eV) from the mica substrate suggests that silicon is a surface contaminant from the annealing process, and XPS did not sample the substrate through the polymer films. Figure 1 shows the XPS C 1s spectra with fitted peaks for spin-cast 50% PS:50% PMMA blend and after annealing at 142 °C for 42 h. These peaks are assigned to the chemical groups found in the PS and PMMA homopolymers.[7,28] The envelope can be resolved into four chemical components: C−C/C−H at 285.0 eV, β-shifted carbon (due to juxtaposition to ester group) at 285.7 eV, methoxy group carbon at 286.8 eV, carbon in ester group at 289.1 eV, and π−π* shake-up satellites at shifts of 6−8 eV. For quantitative analysis of the surface composition for the blend, the PMMA molar concentration at the surface was evaluated by using either the elemental O/C ratio from survey spectra or the percentage of the ester group in the C 1s envelopes. The ester peak at binding energy of 289.1 eV was specially chosen for this purpose because it contains contribution solely from PMMA and does not significantly overlap with any other peak. The experimental O/C ratio contains the contribution of each polymer to the overall O 1s and C 1s spectra, which can be expressed as

$$\left(\frac{O}{C}\right)_{exp} = \frac{XO_{PMMA}}{XC_{PMMA} + (1 - X)C_{PS}} \qquad (1)$$

where X is the molar PMMA surface concentration in the blend and O_{PMMA}, C_{PMMA}, and C_{PS} are respectively the stoichiometric oxygen and carbon atomic concentrations in pure PMMA and pure PS ($O_{PMMA} = 2$, $C_{PMMA} =$

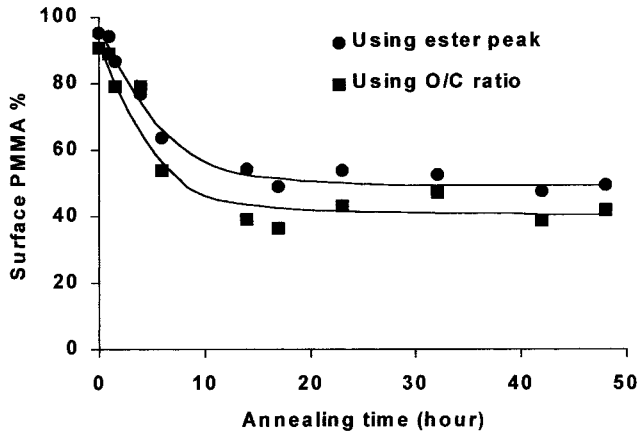

Figure 2. Surface molar concentration of PMMA in the 50% PS:50% PMMA blend calculated by means of elemental O/C ratio (■) and relative ester peak intensity (●) as a function of annealing time. The curves are drawn as a guide only.

5, and $C_{PS} = 8$). Rearranging eq 1, we have

$$X = \frac{8\left(\frac{O}{C}\right)_{exp}}{3\left(\frac{O}{C}\right)_{exp} + 2} \tag{2}$$

Since in the blend the relative contribution of PMMA in the C 1s intensity is $5X$ (five carbon atoms per PMMA repeat unit) and that of PS is $8(1 - X)$ (eight carbon atoms per PS repeat unit), we have

$$\left(\frac{I_{O=C-O}}{I_C}\right)_{exp} = \frac{X}{5X + 8(1 - X)} \tag{3}$$

Rearranging eq 3 gives

$$X = \frac{8\left(\frac{I_{O=C-O}}{I_C}\right)_{exp}}{3\left(\frac{I_{O=C-O}}{I_C}\right)_{exp} + 1} \tag{4}$$

The molar PMMA surface concentration in the 50% PS: 50% PMMA with annealing time, evaluated using the above methods, is shown in Figure 2. Uncertainties of the measured PMMA surface concentrations were estimated at ±10%, which was deduced from the measurements on three different samples. The PMMA concentration determined from the O/C ratio is consistently 5−15% lower than that determined using the ester peak. The discrepancy probably arises from the different XPS sampling depths for O 1s and C 1s photoelectrons and is indicative of a hydrocarbon overlayer. The difference in the sampling depths can result in inaccurate experimentally determined O/C ratios at heterogeneous surfaces; the data set derived from the ester peak is therefore preferentially chosen for reporting the surface PMMA concentrations. The surface overlayer may be either PS or some contamination from the annealing process. An alternative explanation for this discrepancy is orientation of the ester groups of the PMMA in the near surface region. It was found that in most of the annealed samples intensities of the three chemically shifted carbon peaks are not identical as expected from the stoichiometric atomic composition of the PMMA, but decrease in the order of β-shifted carbon > methoxyl carbon > ester carbon.

In Figure 2, PMMA surface concentration decreases with annealing time as determined using either the O/C ratio or ester peak. A gradual decrease in surface PMMA level is observed up to an annealing time of 17 h, after which the level remains almost unchanged at 53 ± 3% as quantified using the ester peak and 42 ± 5% using the O/C ratio. Analysis of the relative intensities of the $\pi-\pi^*$ shake-up satellites from the C 1s peak envelopes also reveals an increase in intensity with annealing time (see Figure 1). This indicates that PS has preferentially segregated to the surface since it has lower surface free energy. The shake-up peaks are difficult to quantify accurately due to their weak signals and the strong dependence of peak area on background selection.

Variable electron takeoff angle XPS was performed to investigate the surface segregation of the PS in the annealed films. Analysis of the annealed films revealed a decrease in PMMA intensity with decreasing sampling depth, as indicated by both the oxygen signal and the ester peak. The PMMA surface concentrations of the 32 h annealed film measured at takeoff angles of 0°, 30°, 45°, and 60° (relative to the sample surface normal) were 54%, 34%, 22%, and 9%, respectively. The sampling depths of the XPS experiment at 0° and 60° takeoff angle are approximately 9.0 and 4.5 nm, respectively.[29] This indicates that the film surface is covered with a single phase of the PS. The results are confirmed by the shake-up peaks, which were observed to increase with lower sampling depth. Attenuation of the PMMA signals at different takeoff angles can give some information whether the thickness of PS layer is homogeneous.[30] Analysis of XPS spectra collected at various takeoff angles reveals that the PMMA signal change did not fit with a thin, flat overlayer model.[21]

Atomic Force Microscopy (AFM). Figure 3 shows 3D AFM images of 50% PS:50% PMMA blend film at the different stages of annealing. For the spin-cast blend film, the AFM topography shows a pitted surface (Figure 3a). The pits have a broad, shallow structure with typical diameters between 1.1 and 1.4 μm and depths of 30−40 nm. The pitted surface structure was observed to remain for over 14 h of annealing, as shown for the films annealed for 4 and 12 h in parts b and c of Figure 3. However, the pits get continually shallower, with depths of 5−20 nm after 4 h of annealing. Small pits appear on the film surfaces of 2−4 h annealing then diminish in size and disappear for longer annealing times. For the film annealed for 12 h, the surface appears relatively flat, but the pits are still identifiable. When the annealing time is increased to above 14 h, the pitted surface tends to be distorted with no defined pit structure (Figure 3d).

In addition to imaging the topography of the blend, frictional force microscopy (FFM) with hydroxylated tips was used to probe the phase structure of film surfaces. Frictional contrast between the two polymers with chemically modified tips has previously shown that differentiation between them is possible.[7,31] Friction measured on the pure PMMA film was higher than that of the pure PS film. This is probably due to polar interactions between the hydroxylated tip and polymer surface, as reported in previous studies.[7,32] For the spin-cast film FFM reveals no contrast between the pits and the surrounding matrix (Figure 4a), suggesting that the

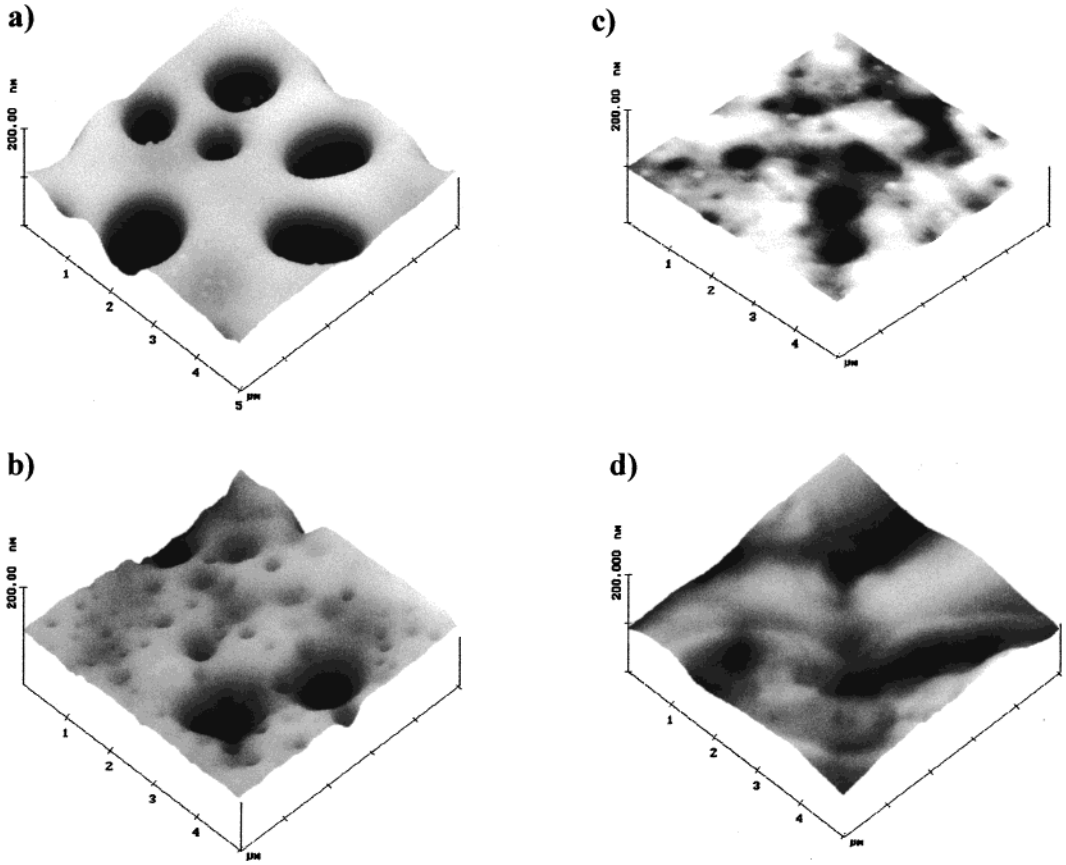

Figure 3. AFM images of PS/PMMA blend films showing changes in surface topography upon annealing: spin-cast (a); after annealing for 4 h (b), 12 h (c), and 42 h (d).

whole surface is composed of a single phase. The top surface layer is PMMA, as indicated by XPS measurement which shows that the PMMA surface concentration is 95 ± 5%. Figure 4b represents topographical and frictional force images of the same film after 2 h of annealing. The frictional image reveals lower friction (dark contrast) within the pits and higher friction (light contrast) in the continuous surface matrix. This indicates that PS-rich domains have formed in the surface pits upon the annealing. In the PS-rich phase small dropletlike domains of PMMA are visible. Additionally, for the films that were annealed for over 14 h, FFM reveals similar contrast over the entire image, as seen in Figure 4c. These observations indicate that the composition of the pits is not significantly different from the surface matrix but that the whole surface of these annealed films consists of a single rich phase.

Discussion

The spin-cast films in these studies possess nonequilibrium surfaces with a significant excess of PMMA. Their surfaces are covered with a PMMA-rich phase although its surface free energy is slightly higher than that of the PS component. During the spin-casting process, since the solvent evaporates relatively fast, the polymer chains are generally frozen in the thin films before attainment of a thermodynamically stable state. The surface enrichment of the PMMA in the cast films probably arises from its higher solubility in the chloroform as discussed in a previous study.[7] Upon annealing above the glass transition temperatures of the two polymers, surface segregation of the PS component occurs in order to minimize the polymer−air interfacial free energy. The surface enrichment was revealed by the XPS measurements, which show that the surface PS concentration increases from ∼5% of the spin-cast films to ∼47% after 17 h of annealing. Thereafter, the surface composition of the films remains unchanged within the depth of the XPS experiment (approximately 9 nm for PS and PMMA at the normal electron takeoff angle[29]). Surface enrichment either pre- or postannealing may be effected by the molecular weight and molecular weight distribution of the polymers. However, the effects of the molecular weights are not the subject of the current investigation.

The changes in surface morphology in the initial annealing stages are caused by the dewetting of PMMA from the PS-rich phase in the surface pits, leading to exposure of the surface PS-rich domains in the pits. Evidence of the small droplets of PMMA in the PS-rich phase suggests that complete phase separation of the two polymers has occurred after the annealing. Longer annealing times (>14 h) resulted in the whole surface composing of a single phase, which is PS-rich as indicated by variable takeoff angle XPS measurements. PMMA observed by XPS in these films is probably subsurface within the sampling depth of the XPS technique. The angle-resolved XPS experiments reveal the decrease of the PMMA signal with increasing takeoff angle, which does not fit with a thin overlayer model,[21] suggesting that continuous but nonhomogeneous layers of PS are generally formed on the annealed film surfaces. In addition to the energetic effects at the polymer−air interface, the increase in the PS surface composition may also be explained by the selective adsorption of the PMMA on the mica substrate. The

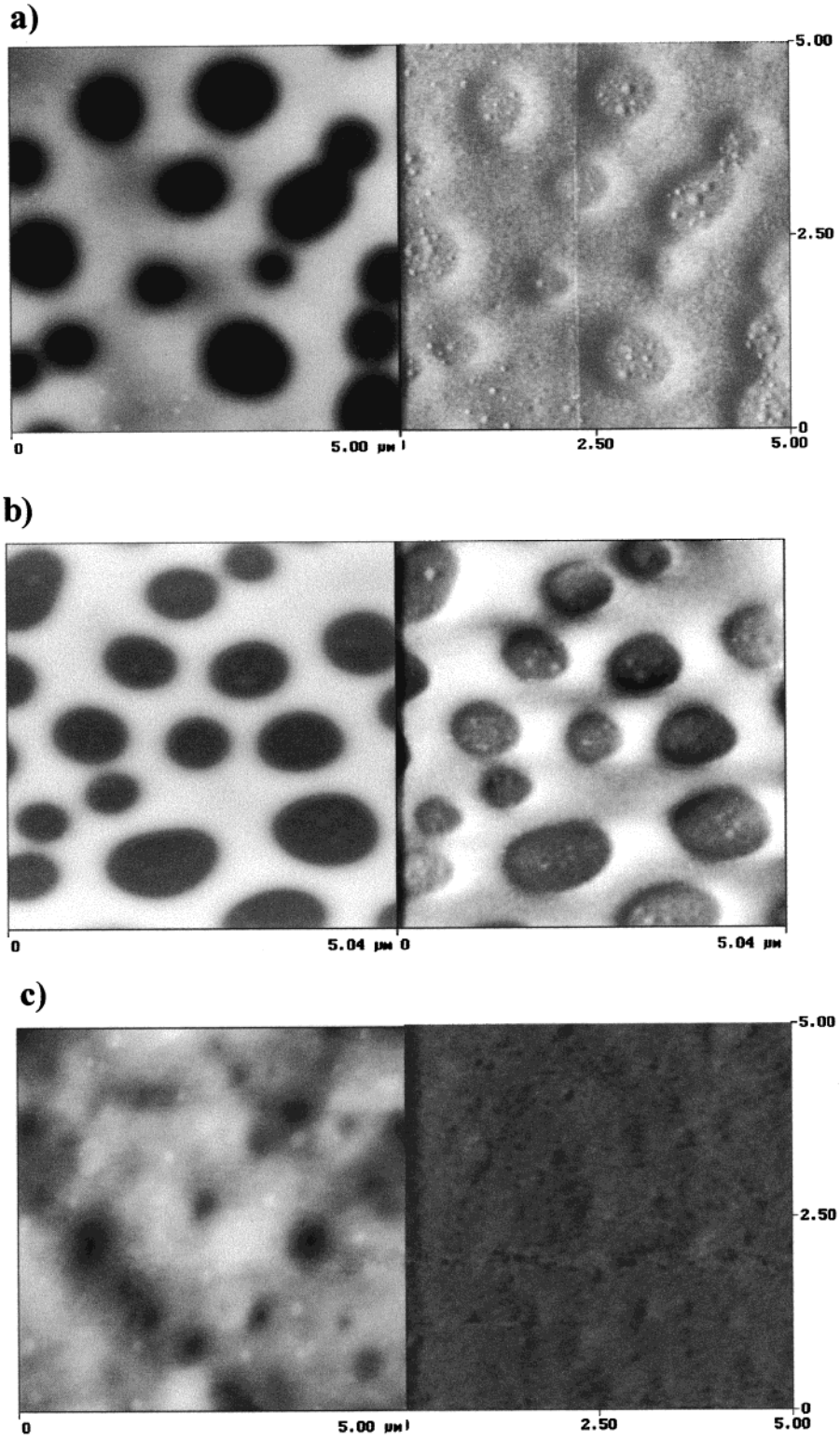

Figure 4. Topographical (left, *z* range = 160 nm) and frictional (right, *z* range = 0.2 V) images of 50% PS:50% PMMA films as spin-casting (a) and after annealing for 2 h (b) and 14 h (c). The images were recorded in fluid (decane) environment using hydroxylated AFM tips.

PMMA with a higher surface free energy is more favorable to adsorb onto the hydrophilic mica (water contact angle $\sim 0°$) to reduce the polymer−substrate interfacial energy. Such selective adsorption of polymers on the substrate has been reported previously for thin (<100 nm) films.[9] The above results have suggested a reversal of surface hierarchy from PMMA-rich to PS-rich surface coverage after annealing for >14 h. This reversal is favorable in terms of energetics, and the resulting surfaces are more stable than those of the spin-cast films.

In theories of liquid/liquid dewetting, the condition of wettability is dictated by the spreading coefficient

$$S = \gamma_2 - (\gamma_1 + \gamma_{12}) \tag{5}$$

where γ_1 and γ_2 are the surface tensions of the two polymers, and γ_{12} is their interfacial tension. For $S > 0$

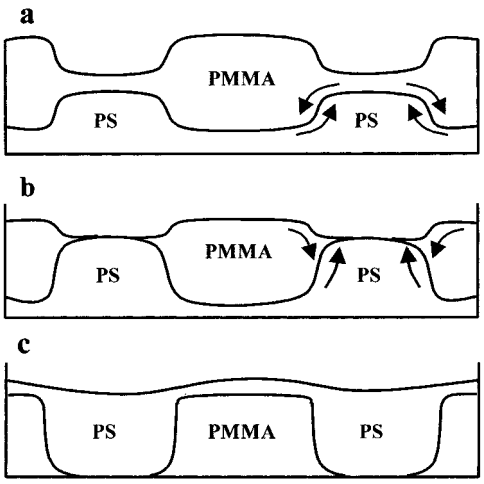

Figure 5. Structural model of PS/PMMA blend as spin-cast (a) and upon annealing above the glass transition temperature in the early stage (b) and later stage (c). Arrows indicate the movements of the PS-rich and PMMA-rich domains at their interface.

the situation of complete wetting occurs, while $S < 0$ corresponds to partial wetting or nonwetting. Assuming that the interface between the two polymers corresponds to the plane of dewetting, there is a negative spreading coefficient of -4.3 mJ/m^2 for PS/PMMA ($\gamma_{PS} = 40.2$ mJ/m^2, $\gamma_{PMMA} = 41.2$ mJ/m^2,[9] and $\gamma_{PS/PMMA} = 3.3$ mJ/m^2 [33]). The dewetting of PMMA from PS-rich phase in the spin-cast films is therefore thermodynamically favorable and consistent with the surface segregation of PS observed upon annealing. The dewetting dynamics of the polymers upon annealing are substantially faster than at room temperature. At the annealing temperature (142 °C), which are well above their glass transition temperatures (106 and 111 °C for PS and PMMA, respectively), the polymers behave like viscous liquids, and polymer segment movements on a large scale are attainable.

The above results lead us to consider a possible model for the blend upon annealing, which is shown in Figure 5a−c. The surface oscillation in Figure 5a represents the longitudinal peristaltic mode in stratified liquids.[34] This oscillation is of importance when dewetting dynamics of a liquid film deposited on a liquid substrate are considered. The pitted structure in the spin-cast films may occur via the initial formation of a bilayer solution of PMMA on top of a PS solution. This is due to a higher solubility of the PMMA in the chloroform, resulting in PMMA staying longer in the liquid phase and forming a second top layer.[7] As the films are annealed at above the glass transition temperatures, the PMMA layer starts to dewet from the PS layer. The dewetting first occurs within the pits where the PMMA overlayer is thinner, leading to formation of surface domains of PS-rich phase as illustrated in Figure 5b. In the intermediate stage of dewetting (between 1.5 and 4 h annealing), FFM with hydroxylated tip was able to probe the phase contrast between the pits and surface matrix. Longer annealing times result in further dewetting and the PS component gradually segregating to the surface to form a continuous overlayer (Figure 5c). Complete phase separation of the polymers occurs in the bulk after annealing, but the whole surface comprises a single PS-rich phase. The behavior of polymer phases in the subsurface is conjectural.

Conclusion

Surface analysis of a 50% PS:50% PMMA blend upon annealing has recorded both surface segregation of PS and topographical changes. This surface segregation probably occurred due to a lower surface free energy of the PS component. The PS molar surface concentration measured by XPS increased from 5% to a saturated level of 47% as evaluated by the ester peak and 58% by the O/C ratio after 17 h of annealing. For the films annealed for 17 h or longer, angle-resolved XPS detected only almost the PS component within the sampling depth of approximately 4 nm. AFM revealed pitted surface topography of the spin-cast blend films. The pitted structure remained on the surface for over 14 h of annealing, but the pit depth gradually decreased. The pitted surface became distorted for longer annealing times above 14 h. FFM with the use of hydroxylated probe tips allowed differentiation of the PS-rich and PMMA-rich surface phases. Surface phase separations were observed for the annealing times of 2−4 h. For the spin-cast films and after annealing for over 14 h, the film surfaces were composed of a single phase. These findings are consistent with a reversal of surface hierarchy from PMMA to PS surface coverage.

Acknowledgment. C.T.T. acknowledges financial support from the Robert Gordon University.

References and Notes

(1) Kajiyama, T.; Tanaka, K.; Takahara, A. *Macromolecules* **1995**, *28*, 3482−3484.
(2) Chiou, J. S.; Barlow, J. W.; Paul, D. R. *J. Polym. Sci., Part B* **1987**, *25*, 1459−1471.
(3) Lhoest, J. B.; Bertrand, P.; Weng, L. T.; Dewez, J. L. *Macromolecules* **1995**, *28*, 4631−4637.
(4) Overney, R. M.; Leta, D. P.; Fetters, L. J.; Liu, Y.; Rafailovich, M. H.; Sokolov, J. *J. Vac. Sci. Technol.* **1996**, *14*, 1276−1279.
(5) Kano, Y.; Akiyama, S.; Kasemura, T. *Int. J. Adhes. Adhes.* **1997**, *17*, 207−212.
(6) Gutmann, J. S.; Muller-Buschbaum, P.; Schubert, D. W.; Stribeck, N.; Stamm, M. *J. Macromol. Sci., Phys.* **1999**, *B38*, 563−576.
(7) Ton-That, C.; Shard, A. G.; Teare, D. O. H.; Bradley, R. H. *Polymer* **2000**, *42*, 1121−1129.
(8) Davies, M. C.; Shakesheff, K. M.; Shard, A. G.; Domb, A.; Roberts, C. J.; Tendler, S. J. B.; Williams, P. M. *Macromolecules* **1996**, *29*, 2205−2212.
(9) Tanaka, K.; Takahara, A.; Kajiyama, T. *Macromolecules* **1996**, *29*, 3232−3239.
(10) Tanaka, K.; Takahara, A.; Kajiyama, T. *Macromolecules* **1995**, *28*, 934−938.
(11) Schmidt, J. J.; Gardella, J. A.; Salvati, L. *Macromolecules* **1989**, *22*, 4489−4495.
(12) Lim, D. S.; Kyu, T. *J. Chem. Phys.* **1990**, *92*, 3944−3950.
(13) Kajiyama, T.; Tanaka, K.; Takahara, A. *Macromolecules* **1998**, *31*, 3746−3749.
(14) Garbassi, F.; Morra, M.; Occhiello, E. *Polymer Surfaces: from Physics to Technology*; John Wiley & Sons: Chichester, 1998; p 291.
(15) Green, P. F.; Christensen, T. M.; Russell, T. P.; Jerome, R. *J. Chem. Phys.* **1990**, *92*, 1478−1482.
(16) Schwarz, S. A.; Wilkens, B. J.; Pudensi, M. A. A.; Rafailovich, M. H.; Sokolov, J.; Zhao, X.; Zhao, W.; Zheng, X.; Russell, T. P.; Jones, R. A. L. *Mol. Phys.* **1992**, *76*, 937−950.
(17) Affrossman, S.; Hartshorne, M.; Kiff, T.; Pethrick, R. A.; Richards, R. W. *Macromolecules* **1994**, *27*, 1588−1591.
(18) Jones, R. A. L.; Kramer, E. J.; Rafailovich, M. H.; Sokolov, J.; Schwarz, S. A. *Phys. Rev. Lett.* **1989**, *62*, 280−283.
(19) Chen, X.; Lee, H. L.; Gardella, J. A. *Macromolecules* **1993**, *26*, 4601−4605.
(20) Limary, R.; Green, P. F. *Macromolecules* **1999**, *32*, 8167−8172.
(21) Ton-That, C.; Shard, A. G.; Bradley, R. H. *Langmuir* **2000**, *16*, 2281−2284.

(22) Ito T.; Namba, M.; Buhlmann, P.; Umezawa, Y. *Langmuir* **1997**, *13*, 4323−4332.
(23) Vig, J. R. *J. Vac. Sci. Technol. A* **1985**, *3*, 1027−1034.
(24) Ogbuji, L. U. T.; Jayne, D. T. *J. Electrochem. Soc.* **1993**, *140*, 759−766.
(25) Digital Instruments, Santa Barbara, CA.
(26) Grigg, D. A.; Russel, P. E.; Griffith, J. E. *J. Vac. Sci. Technol. A* **1992**, *10*, 680−683.
(27) Feldman, K.; Tervoort, T.; Smith, P.; Spencer, N. D. *Langmuir* **1998**, *14*, 372−378.
(28) Beamson, G.; Briggs, D. *High-Resolution XPS of Organic Polymers*; John Wiley & Sons: Chichester, 1992.
(29) Lukas, J.; Jezek, B. *Collect. Czech. Chem. Commun.* **1983**, *48*, 2909−2913.
(30) Briggs, D.; Riviere, J. C. In *Practical Surface Analysis;* Briggs, D., Seah, M. P., Eds.; Wiley: Chichester, 1995, Vol. 1, p 134.
(31) Krausch, G.; Hipp, M.; Boltau, M.; Marti, O.; Mlynek, J. *Macromolecules* **1995**, *28*, 260−263.
(32) Ton-That, C.; Campbell, P. A.; Bradley, R. H. *Langmuir* **2000**, *16*, 5054−5058.
(33) Paul, D. R.; Newman, S. *Polymer Blends*; Academic Press: New York, 1978; p 277.
(34) Brochard-Wyart, F.; Martin, P.; Redon, C. *Langmuir* **1993**, *9*, 3682−3690.

MA000792H